

Benzylideneruthenium Complexes Bearing Pyridine-Based Ligands and Their Influence on the Formation of Mono- or Bis(pyridine) Complexes

Wen-Zhen Zhang,^[a] Ren He,^{*[a]} and Rong Zhang^[a]

Keywords: Metathesis / Ruthenium / N ligands / Ligand effects / Homogeneous catalysis

Benzylideneruthenium complexes bearing the N-heterocyclic carbene (NHC) ligand 1,3-bis(2,6-dimethylphenyl)-4,5-dihydroimidazol-2-ylidene (H₂IMe) and one or two pyridine-based ligands have been prepared by treating [RuCl₂(=CHPh)(H₂IMe)(PPh₃)] with the corresponding pyridine derivative. X-ray crystallographic and mass spectrometric evidence is used to investigate the interconversion between mono- and bis(pyridine) complexes and the influence of the

pyridine ligand on the formation of these complexes. The catalytic activity of these complexes has been tested in the ring-closing metathesis (RCM) reaction of diallylmalononitrile and the cross metathesis (CM) reaction of acrylonitrile with terminal olefins.

(© Wiley-VCH Verlag GmbH & Co. KGaA, 69451 Weinheim, Germany, 2007)

Introduction

Alkylideneruthenium complexes, which exhibit remarkable air and water stability and significant functional-group tolerance, have been applied extensively as efficient metathesis catalysts in organic synthesis and polymer chemistry.^[1] In particular, the second-generation Grubbs catalyst,^[2] which contains a saturated NHC ligand instead of one of the PCy₃ ligands of the first-generation Grubbs catalyst,^[3] exhibits a dramatically enhanced catalytic activity.^[4] Further substitution of the PCy₃ ligand in the second-generation Grubbs catalyst with pyridine or 3-bromopyridine has resulted in the successful development of fast-initiating catalysts **I**^[5] and **II**^[6] (Figure 1). The alkylidene complex **IV**, analogous to complex **II**, is also a fast initiator of olefin metathesis.^[7]

With regard to catalysts **I–IV**, bis(pyridine) complexes are considered to be formed preferentially to mono(pyridine) complexes. The solid-state structures of bis(pyridine) complexes **I** and **IV** have been confirmed by X-ray crystallography, although Grubbs has also observed that the mono(pyridine) complex [RuCl₂(=CHPh)(H₂IMes)(C₅H₅N)] can be formed by recrystallizing complex **I** and then drying it under vacuum. This implies that the six-coordinate bis(pyridine) complex **I** can easily lose pyridine under vacuum to give the five-coordinate mono(pyridine) complex.^[5]

Five-coordinate benzylidene mono(pyridine)ruthenium complexes can be obtained exclusively under certain circumstances. Thus, the reaction of complex **I** with NaI affords the benzylidenediiodoruthenium complex **V** with a single pyridine ligand rather than the corresponding bis(pyridine) complex, probably due to the relatively large size of the iodido ligands and the lower electrophilicity at the metal center.^[5] Fogg has reported that modification of the anionic ligands of [RuCl₂(=CHPh)(IMes)(Py)₂] with aryl-oxido ligands also results in a series of five-coordinate benzylidene mono(pyridine)ruthenium catalysts (**VII–XI**).^[8] X-ray crystallographic analysis of complex **VII** clearly showed mono(pyridine) coordination, presumably because of steric hindrance.^[8a] Similarly, Buchmeiser et al. have reported that treatment of [RuCl₂(=CHPh)(Mes₂-THP)(PCy₃)] (Mes₂-THP = 1,3-dimesityltetrahydropyrimidin-2-ylidene) with an excess of pyridine gives the mono(pyridine) complex **VI**, which they tentatively attributed to the increased donor capability and steric hindrance of the Mes₂-THP ligand compared to H₂IMes.^[9] Accordingly, the steric and electronic properties of the NHC and anionic ligands around the metal center have a pronounced effect on the formation of mono- or bis(pyridine) complexes. The influence of the pyridine ligand on the formation of mono- or bis(pyridine) complexes has rarely been investigated, however.

Herein we describe the synthesis, X-ray crystallographic structures and mass spectrometric behavior of benzylideneruthenium complexes containing various pyridine ligands and the interconversion between mono- and bis(pyridine) complexes. These studies provide some insight into how the pyridine ligands influence the formation of mono- or bis(pyridine) complexes. Additionally, the catalytic ac-

[a] State Key Laboratory of Fine Chemicals, Dalian University of Technology (DUT), 158 Zhongshan Rd., 116012 Dalian, China
Fax: +86-411-83633080
E-mail: beyoudutmost@yahoo.com.cn

Supporting information for this article is available on the WWW under <http://www.eurjic.org> or from the author.

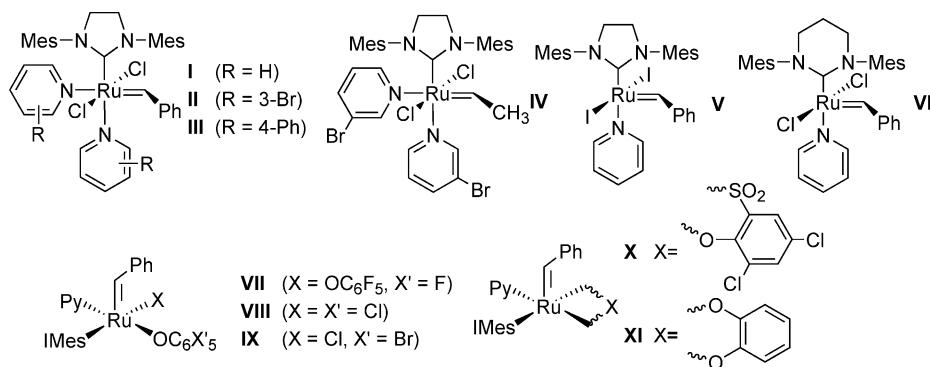


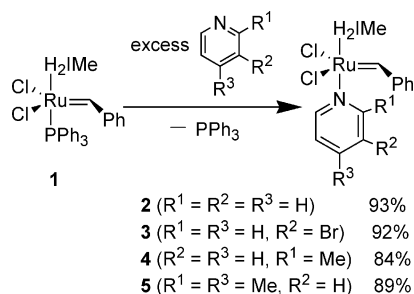
Figure 1. Benzylidenebis- and -mono(pyridine)ruthenium complexes used as metathesis catalysts (IMes = 1,3-dimesitylimidazol-2-ylidene; Mes = 2,4,6-trimethylphenyl).

tivity of these complexes is tested in the ring-closing metathesis (RCM) reaction of diallylmalononitrile and the cross metathesis (CM) reaction of acrylonitrile with terminal olefins.

Results and Discussion

Synthesis and X-ray Crystallography

Benzylideneruthenium complexes **2–7** were prepared in good yield by treating $[\text{RuCl}_2(\text{=CHPh})(\text{H}_2\text{IMe})(\text{PPh}_3)]$ (**1**)^[10] with the corresponding pyridine derivative according to the procedure described by Grubbs (Scheme 1).^[5,6] Complex **1**, which bears a PPh_3 ligand instead of the PCy_3 ligand of the second-generation Grubbs catalyst, was used in this reaction because dissociation of the PPh_3 ligand in complex **1** proved to be easier than that of PCy_3 in the Grubbs catalyst.^[11] Complex **2**, which contains a more labile ligand, was found to be unsuitable as a precursor for the synthesis of other complexes containing pyridine-based ligands because of the difficulty in separating the two complexes.



Scheme 1. Synthesis of mono(pyridine) complexes.

Complexes **2** and **3** are easily accessible, although the synthesis of complexes **4** and **5**, which contain an *ortho*-substituted pyridine ligand to weaken the coordination of the pyridine ligand to the ruthenium atom and accelerate initiation through steric hindrance, proved time-consuming and relatively difficult to perform. The reaction of complex **1** with 2,6-dimethylpyridine, quinoline, or 2-bromopyridine failed to yield the corresponding complexes, probably due

to an excessive weakening of the coordinating ability of these pyridine-based ligands.

The ^1H NMR spectroscopic and mass spectrometric data of complexes **2–5** suggested that they are mono(pyridine) complexes. Complexes **2**, **4**, and **5** were investigated by X-ray crystallography to confirm their five-coordinate mono(pyridine) structure. Crystals suitable for X-ray analysis were obtained by slow diffusion of pentane into saturated chloroform/hexane (for complexes **2** and **5**) or dichloromethane/hexane (for complex **4**) solutions of the complexes. Crystals of complex **3** suitable for X-ray analysis could not be obtained. The crystal structures of complexes **2**, **4**, and **5** are shown in Figures 2, 3, and 4, respectively. Selected bond lengths and angles are summarized in Table 1, and crystal data and other details of the structure analysis are given in the Experimental Section.

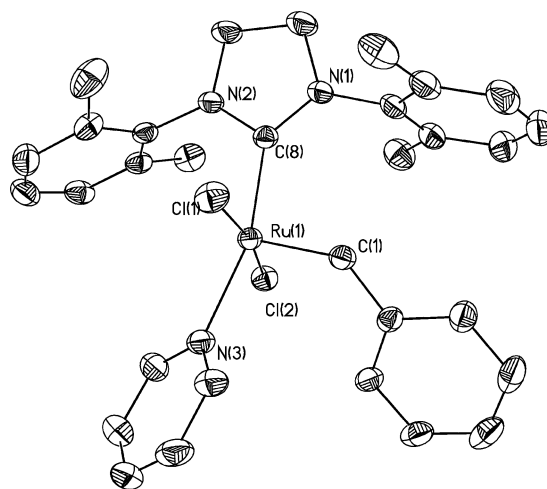


Figure 2. Molecular structure of **2** with thermal ellipsoids drawn at the 30% probability level. Hydrogen atoms have been omitted for clarity.

X-ray analysis confirmed that complexes **2**, **4**, and **5** are five-coordinate mono(pyridine) complexes. The coordination geometries of these complexes are distorted square pyramids with the two chlorido ligands and the pyridine and NHC ligands in a mutually *trans* arrangement and the apical positions occupied by the benzylidene ligands. The

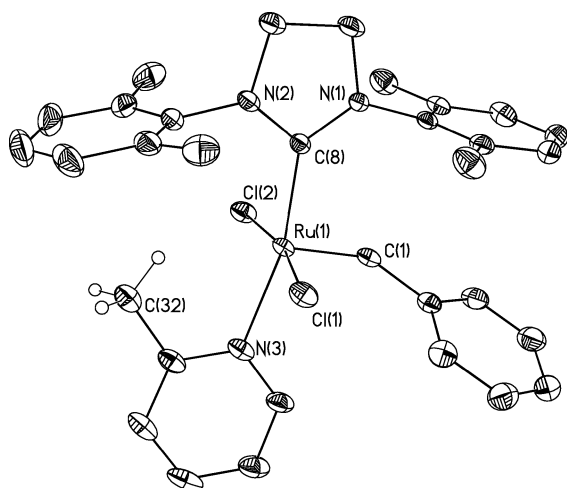


Figure 3. Molecular structure of **4** with thermal ellipsoids drawn at the 30% probability level. Most hydrogen atoms have been omitted for clarity.

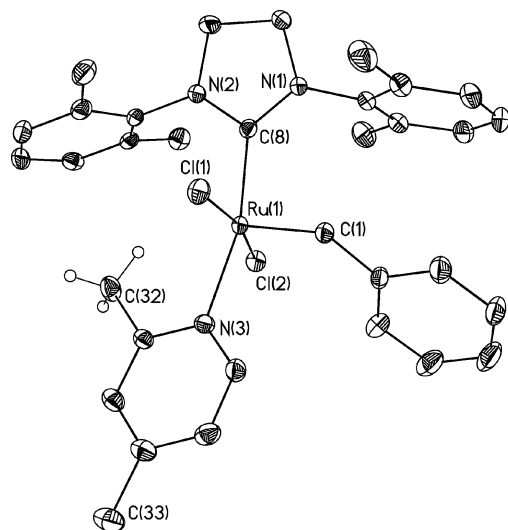


Figure 4. Molecular structure of **5** with thermal ellipsoids drawn at the 30% probability level. Most hydrogen atoms have been omitted for clarity.

Ru–N(3) bonds of **4** [2.165(3) Å] and **5** [2.160(3) Å] are longer than that of **2** [2.156(2) Å], which suggests a weaker interaction between the ruthenium atom and the pyridine ligands in complexes **4** and **5** due to the steric hindrance of the *ortho*-methyl group. The fact that the Ru–C(8) (N-heterocyclic carbene) bonds of **4** [2.042(3) Å] and **5** [2.043(3) Å] are longer than that of **2** [2.025(3) Å] is likely due to the relatively moderate *trans* effects of *ortho*-substituted pyridines, which also reflects the trend of the Ru–N(3) bond lengths. Complex **5** has slightly shorter Ru–N(3) and longer Ru–C(8) bond than complex **4**, which can be attributed to the electron-donating effect of the *para*-methyl group in the 2,4-dimethylpyridine ligand. The dihedral angles between the NHC ring and the pyridine ring of **4** (11.7°) and **5** (23.0°) are narrower than that of **2** (42.1°), and the C(8)–Ru–N(3) angles of **4** [165.45(14)°] and **5** [165.62(14)°] are slightly wider than that of **2** [163.82(10)°], both of which might be due to the steric demands of the *ortho*-methyl group in the pyridine ligand of complexes **4** and **5**. Accordingly, it can be concluded that the steric demand of the *ortho*-methyl group in the pyridine ligand plays a crucial role in the formation of five-coordinate mono(pyridine) complexes **4** and **5**.

Additionally, the ruthenium centers in complexes **4** and **5** do not appear to have the agostic interactions that are known to stabilize four-coordinate 14-electron ruthenium(II) complexes as the closest Ru⋯C [other than C(1) and C(8); 3.04 Å for **4** and 3.03 Å for **5**] and Ru⋯H distances (other than H_{carbene}; 2.37 Å for **4** and **5**) are all too long for an agostic interaction.^[12]

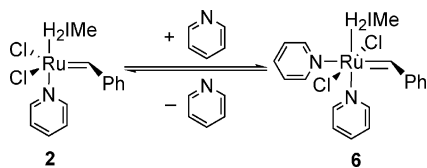
Interconversion between Mono- and Bis(pyridine) Complexes

As described by Grubbs, the bis(pyridine) complex **6** can also change into the mono(pyridine) complex **2** upon loss of one pyridine ligand under vacuum, and complex **2** can easily revert into complex **6** in the presence of an excess of pyridine (Scheme 2). For instance, a crystal of complex

Table 1. Selected bond lengths [Å] and angles [°] for complexes **2** and **4–7**.

	2	4	5	6	7
Ru–C(1)	1.829(3)	1.836(4)	1.838(4)	1.867(6)	1.860(5)
Ru–C(8)	2.025(3)	2.042(3)	2.043(4)	2.053(6)	2.060(5)
Ru–N(3)	2.156(2)	2.165(3)	2.160(3)	2.205(5)	2.207(4)
Ru–N(4)				2.367(5)	2.359(4)
Ru–Cl(1)	2.3844(7)	2.3749(10)	2.3873(12)	2.4275(16)	2.4379(14)
Ru–Cl(2)	2.3636(7)	2.4081(10)	2.3864(11)	2.3912(17)	2.3740(13)
C(8)–Ru–C(1)	97.42(12)	95.06(15)	94.91(17)	94.1(2)	94.8(2)
C(8)–Ru–N(3)	163.82(10)	165.45(14)	165.62(14)	178.95(19)	177.52(18)
C(8)–Ru–N(4)				101.91(19)	101.92(17)
C(8)–Ru–Cl(1)	89.51(8)	91.44(10)	88.29(12)	88.22(17)	90.08(15)
C(8)–Ru–Cl(2)	93.58(8)	92.68(10)	95.60(12)	90.75(17)	88.02(15)
C(1)–Ru–N(3)	98.33(11)	99.48(14)	97.70(16)	86.7(2)	87.54(19)
C(1)–Ru–N(4)				161.2(2)	161.98(19)
C(1)–Ru–Cl(1)	90.57(9)	102.06(13)	88.70(15)	83.81(19)	84.78(17)
C(1)–Ru–Cl(2)	97.46(9)	88.09(13)	101.14(15)	100.39(19)	98.15(17)
Cl(1)–Ru–Cl(2)	170.94(3)	168.67(4)	169.04(4)	175.74(6)	176.62(5)

6 suitable for X-ray analysis can be obtained by slow diffusion of pentane into a chloroform/hexane solution of complex **2** (10 mg) and pyridine (0.1 mL, approx. 75 equiv.). Figure 5 illustrates the molecular structure of complex **6**, and Table 1 summarizes selected bond lengths and angles. Crystal data and other details of the structure analysis are presented in the Experimental Section.



Scheme 2. Interconversion between mono(pyridine) complex **2** and bis(pyridine) complex **6**.

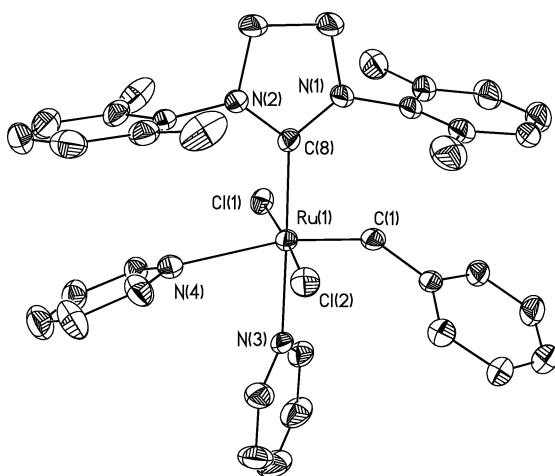
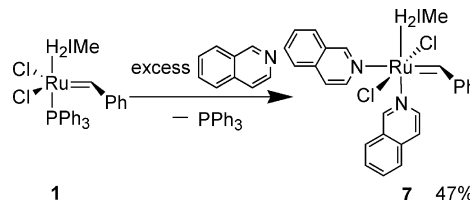


Figure 5. Molecular structure of **6** with thermal ellipsoids drawn at the 30% probability level. Hydrogen atoms have been omitted for clarity.

Complex **6** has a pseudo-octahedral geometry with the two chlorido ligands in a *trans* arrangement and two pyridine ligands in a mutually *cis* arrangement and *trans* to the NHC and the benzylidene ligand, respectively. The Ru–C, Ru–N, and Ru–Cl bonds in complex **6** are all longer than in complex **2**, presumably due to the increased steric demand and relatively lower electrophilicity at the metal center when another pyridine ligand is introduced *trans* to the benzylidene ligand. Similarly, the C(8)–Ru–N(3) and Cl(1)–Ru–Cl(2) angles are widened to 178.95(19)° and 175.74(6)°. The Ru–N(4) [2.367(5) Å] bond in complex **6** is 0.16 Å longer than Ru–N(3) [2.205(5) Å], which implies that the pyridine ligand *trans* to the benzylidene ligand is more likely to dissociate than the pyridine ligand *trans* to the NHC ligand. Removal of the pyridine ligand *trans* to the benzylidene ligand in bis(pyridine) complex **6** can therefore be easily carried out to form mono(pyridine) complex **2** under certain circumstances, for example under vacuum or in solution. The pyridine ligand in complex **2** is relatively difficult to remove because the Ru–N(3) interaction is strengthened, whereas the steric environment and relatively higher electrophilicity at the metal center allow for the association

of one pyridine ligand at the coordination site *trans* to the benzylidene ligand.

Interestingly, treatment of complex **1** with an excess of isoquinoline gives the six-coordinate bis(isoquinoline) complex **7** even after drying the product under vacuum for 24 h (Scheme 3). Crystals of complex **7** suitable for X-ray analysis were obtained by slow diffusion of pentane into a saturated chloroform/hexane solution of the complex. As shown in Figure 6 and Table 1, the molecular structure of complex **7** is similar to that of complex **6**. The Ru–N(4) [2.359(4) Å] bond is 0.15 Å longer than Ru–N(3) [2.207(4) Å], which means that the isoquinoline ligand *trans* to the benzylidene ligand is more likely to dissociate than the isoquinoline ligand *trans* to the NHC ligand. The Ru–N(4) bond of **7** [2.359(4) Å] is shorter than that of **6** [2.367(5) Å], which suggests that the interaction between the ruthenium atom and the isoquinoline ligand *trans* to the benzylidene ligand in complex **7** is stronger than the interaction between the ruthenium atom and the pyridine ligand *trans* to the benzylidene ligand in complex **6**. Additionally, the saturated vapor tension of isoquinoline is lower than that of pyridine, which means that bis(isoquinoline) complex **7** cannot be converted into the corresponding five-coordinate mono(isoquinoline) complex under vacuum. However, this conversion can easily be carried out under other conditions, for example in solution.



Scheme 3. Synthesis of bis(isoquinoline) complex **7**.

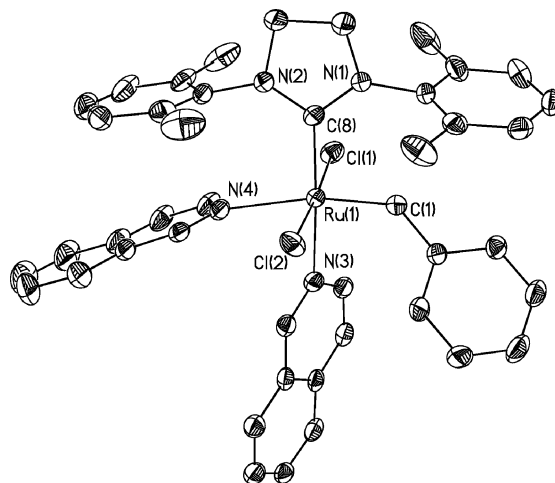


Figure 6. Molecular structure of **7** with thermal ellipsoids drawn at the 30% probability level. Hydrogen atoms have been omitted for clarity.

Mass Spectrometric Study

Tandem mass spectrometry^[13] can be performed when the complexes are delivered to the ionization source in

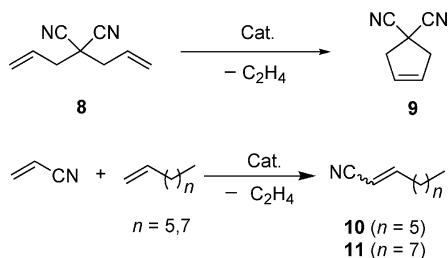
CH₂Cl₂/CH₃CN solution and the collision cone voltages are changed sequentially. All mass spectra are available as Supporting Information. At collision cone voltages of 3 V the [M – Cl + CH₃CN]⁺ cations are found as base peaks for complexes **2** and **3**, which indicates that the pyridine ligands are still bound to the metal center. However, the base peak for complex **4** is the [M – Cl – py + 2 CH₃CN]⁺ cation under the same conditions, which means that 2-methylpyridine has dissociated from the metal center and CH₃CN has occupied the vacant coordination site. The different behaviors of these complexes show the different labilities of their ligands. Thus, the 2-methylpyridine ligand in complex **4** dissociates more easily than the pyridine ligands in complexes **2** and **3**. The dissociation of all pyridine ligands in complexes **2–4** was found to be easier than that of PPh₃ in complex **1**, which is consistent with the different initiation rates determined by NMR spectroscopy or UV/Vis kinetic studies.^[6]

The mono(isoquinoline) species [M – Cl – quinoline + CH₃CN]⁺ was found as the base peak for the bis(isoquinoline) complex **7** (collision cone voltage: 3 V), which suggests that one of the isoquinoline ligands in complex **7** is prone to dissociate under these conditions.

When complex **1** is delivered to the ionization source in CH₂Cl₂/pyridine solution, the bis(pyridine) species [M – Cl – PPh₃ + 2 pyridine]⁺ is detected, whereas, when complex **4** is delivered to the ionization source in CH₂Cl₂/2-methylpyridine/CH₃CN solution, no bis(pyridine) species is found and the [M – Cl + CH₃CN]⁺ cation is the base peak. This suggests that a bis(pyridine) complex can be formed in the presence of excess pyridine, whereas a bis(2-methylpyridine) complex cannot be formed even in the presence of an excess of 2-methylpyridine, probably due to steric hindrance from the *ortho*-methyl group.

Metathesis Activity

The catalytic activities of complexes **2–5** and **7** were tested in the RCM reaction of diallylmalononitrile and the CM reaction of acrylonitrile with terminal olefins (Scheme 4).^[14]



Scheme 4. RCM of diallylmalononitrile and CM of acrylonitrile with terminal olefins.

Studies by Grubbs have suggested that the catalyst efficiency during metathesis of cyano-containing olefin is related to dissociation rate of the ligands.^[6] As shown in Tables 2 and 3, complex **4** has a higher catalytic activity

than the other complexes as either dissociation of the sterically hindered 2-methylpyridine ligand is rapid and/or re-binding of it is slow.

Table 2. RCM reaction of diallylmalononitrile.^[a]

Catalyst	Cat. [mol-%]	Time [h]	Conversion [%] ^[b]
1	5	12	44
2	1	1	70
3	0.5	1	95
4	0.5	<0.5	99
4	0.2	1	96
5	0.5	1	93
5	0.2	1	90
7	0.5	1	79

[a] 0.1 M diallylmalononitrile in CH₂Cl₂ at 40 °C. [b] Conversion was determined by GC and confirmed by ¹H NMR spectroscopy.

Table 3. CM reaction between acrylonitrile and α -olefins.^[a]

Catalyst	<i>n</i>	Yield [%] ^[b]	<i>E/Z</i> ^[c]
2	5	56	1:3.2
3	5	75	1:2.1
4	5	81	1:2.8
5	5	70	1:3.0
7	5	57	1:2.9
2	7	67	1:3.0
3	7	83	1:1.9
4	7	95	1:2.9
5	7	76	1:3.0
7	7	49	1:3.1

[a] 0.1 M acrylonitrile (1.0 equiv.) in CH₂Cl₂, α -olefin (2.0 equiv.), catalyst (2 mol-%), 40 °C, 12 h. [b] Yield of isolated product. [c] Ratios determined by ¹H NMR spectroscopy.

Addition of 10 equiv. of pyridine (relative to complex **2**) to the mixture of the RCM reaction of **8** catalyzed by complex **2** (Table 2) did not alter the conversion, which suggests that the catalytic activity of bis(pyridine) complex **6** is the same as that of mono(pyridine) complex **2**. The 16-electron mono(pyridine) complex **2** loses a pyridine ligand to form the 14-electron catalytically active intermediate, therefore the process whereby the 18-electron bis(pyridine) complex **6** converts into the 16-electron mono(pyridine) complex **2** must occur so fast that it can be neglected.

Conclusions

Benzylideneruthenium complexes containing pyridine-based ligands have been prepared by treating complex **1** with various pyridine ligands. The steric demands of these pyridine ligands play a crucial role in the formation of mono- or bis(pyridine) complexes: *ortho*-substituted pyridine ligands form five-coordinate mono(pyridine) complexes whereas pyridine ligands without *ortho* substituents form both six-coordinate bis(pyridine) complexes and five-coordinate mono(pyridine) complexes. The bis- and mono(pyridine) complexes can interconvert under certain circumstances by loss or association of the pyridine ligand *trans* to the benzylidene ligand. This interconversion has very little effect on the catalytic activities of these complexes. The *ortho* substituents of the pyridine ligands can weaken the

interaction between the ruthenium center and the ligands due to steric hindrance and therefore accelerate the dissociation of these ligands, which enhances the initiation of the catalysts. Complex **4**, which bears a 2-methylpyridine ligand, exhibits the highest catalytic activity for the RCM reaction of diallylmalononitrile and the CM reaction of acrylonitrile with terminal olefins, of complexes **2–5** and **7**.

Experimental Section

General Procedures: Oxygen- and/or moisture-sensitive materials were manipulated using standard Schlenk techniques under dry nitrogen. NMR spectra were recorded with a Varian Inova instrument (400 MHz for ^1H , 160 MHz for ^{31}P , 100 MHz for ^{13}C). High-resolution mass spectra were recorded with a Q-TOF mass spectrometer (Micromass, England) equipped with a Z-spray ionization source. GC analyses were performed with a Hewlett–Packard HP 6890 equipped with an FID and an HP-5 column. Pyridine, 3-bromopyridine, 2-methylpyridine, 2,4-dimethylpyridine, and acrylonitrile were freshly distilled before use. Ruthenium complex **1**^[9] and diallylmalononitrile^[15] were prepared according to literature procedures. Dichloromethane was dried with CaH_2 , distilled, and stored under nitrogen, whereas thf, toluene, and hexane were dried and distilled from Na/benzophenone. All other reagents were of analytical grade, were purchased commercially, and used as received, unless noted otherwise.

[RuCl₂(=CHPh)(H₂Ime)(C₅H₅N)] (2): Pyridine (10.0 mL, 0.124 mol) was added to complex **1** (1.10 g, 1.37 mmol) in a 150-mL Schlenk flask; no additional solvent was required. The reaction mixture was stirred at room temperature for 10 min, during which time a color change from red-brown to green was observed. Hexane (120 mL) was then added at room temperature and a green solid precipitated. This precipitate was filtered, washed four times with 10 mL of hexane, and dried in vacuo for 6 h to afford **2** as a green powder (0.79 g, 93% yield). ^1H NMR (400 MHz, CDCl_3): δ = 19.12 (s, 1 H, Ru=CHPh), 8.64 (br. s, 2 H, pyridine), 7.79–6.93 (multiple peaks, 14 H, pyridine, *ortho* CH, *para* CH, *meta* CH, 2,6-dimethylphenyl aromatic CH), 4.13 (s, 4 H, $\text{NCH}_2\text{CH}_2\text{N}$), 2.67 (br. s, 6 H, *ortho* CH₃), 2.32 (br. s, 6 H, *ortho* CH₃) ppm. ^{13}C NMR (CDCl_3 , 100 MHz): δ = 307.32 (m, Ru=CHPh), 220.41 [s, Ru–C(N)₂], 152.23, 150.44, 136.70, 136.08, 130.64, 130.29, 129.65, 129.04, 128.41, 128.13, 124.04, 123.80, 48.32, 22.85, 18.69 ppm.

[RuCl₂(=CHPh)(H₂Ime)(3-Br-C₅H₄N)] (3): 3-Bromopyridine (6.0 mL, 62.1 mmol) was added to complex **1** (1.90 g, 2.37 mmol) in a 150-mL Schlenk flask; no additional solvent was required. The reaction mixture was stirred at room temperature for 20 min, during which time a color change from red-brown to green was observed. Hexane (120 mL) was then added at room temperature and a green solid precipitated. The flask was sealed under nitrogen and allowed to stand at 0 °C overnight. The green precipitate was then filtered, washed four times with 10 mL of hexane, and dried in vacuo for 6 h to afford **3** as a green powder (1.53 g, 92% yield). ^1H NMR (400 MHz, CDCl_3): δ = 19.05 (s, 1 H, Ru=CHPh), 8.74 (br. s, 1 H, pyridine), 8.59 (br. s, 1 H, pyridine), 7.90–7.04 (multiple peaks, 13 H, pyridine, *ortho* CH, *para* CH, *meta* CH, 2,6-dimethylphenyl aromatic CH), 4.13 (s, 4 H, $\text{NCH}_2\text{CH}_2\text{N}$), 2.63 (br. s, 6 H, *ortho* CH₃), 2.36 (br. s, 6 H, *ortho* CH₃) ppm. ^{13}C NMR (CDCl_3 , 100 MHz): δ = 316.34 (m, Ru=CHPh), 216.63 [s, Ru–C(N)₂], 152.73, 151.48, 148.13, 138.80, 134.57, 132.23, 132.13, 130.33, 130.26, 128.85, 128.09, 127.04, 124.57, 120.78, 51.46, 20.58, 18.93 ppm. C₃₁H₃₂BrCl₂N₃Ru (698.5): calcd. C 53.31, H 4.62, N 6.02; found C 53.12, H 4.59, N 6.07.

[RuCl₂(=CHPh)(H₂Ime)(2-Me-C₅H₄N)] (4): 2-Methylpyridine (6.0 mL, 60.8 mmol) was added to complex **1** (0.50 g, 0.62 mmol) in a 150-mL Schlenk flask; no additional solvent was required. The reaction mixture was stirred at room temperature for 12 h, during which time a color change from red-brown to green was observed. Hexane (100 mL) was then added at room temperature and a green solid precipitated. The flask was sealed under nitrogen and allowed to stand at 0 °C overnight. The green precipitate was then filtered, washed four times with 10 mL of hexane, and dried in vacuo for 6 h to afford **4** as a green powder (0.33 g, 84% yield). ^1H NMR (400 MHz, CDCl_3): δ = 19.64 (s, 1 H, Ru=CHPh), 8.49 (br. s, 1 H, pyridine), 8.01 (br. s, 1 H, pyridine), 7.57–7.02 (multiple peaks, 7 H, pyridine, *ortho* CH, *para* CH, *meta* CH), 6.82 (br. s, 4 H, 2,6-dimethylphenyl aromatic CH), 6.55 (br. s, 2 H, 2,6-dimethylphenyl aromatic CH), 4.16 (s, 2 H, $\text{NCH}_2\text{CH}_2\text{N}$), 3.95 (s, 2 H, $\text{NCH}_2\text{CH}_2\text{N}$), 2.76 (br. s, 9 H, pyridine CH₃, *ortho* CH₃), 2.25 (s, 6 H, *ortho* CH₃) ppm. ^{13}C NMR (CDCl_3 , 100 MHz): δ = 312.64 (m, Ru=CHPh), 218.09 [s, Ru–C(N)₂], 159.53, 151.74, 151.34, 140.53, 139.08, 137.94, 137.75, 137.28, 136.59, 130.91, 130.33, 129.35, 128.99, 128.76, 128.67, 128.33, 128.04, 127.80, 127.62, 126.49, 125.17, 121.32, 120.93, 51.76, 50.85, 31.58, 20.34, 18.41 ppm.

[RuCl₂(=CHPh)(H₂Ime)(2,4-Me₂-C₅H₃N)] (5): 2,4-Dimethylpyridine (2.0 mL, 17.2 mmol) was added to complex **1** (0.14 g, 0.17 mmol) in a 150-mL Schlenk flask; no additional solvent was required. The reaction mixture was stirred at room temperature for 2 h, during which time a color change from red-brown to green was observed. Hexane (100 mL) was then added at room temperature and a green solid precipitated. The green precipitate was filtered, washed four times with 10 mL of hexane, and dried in vacuo for 6 h to afford **5** as a green powder (0.10 g, 89% yield). ^1H NMR (400 MHz, CDCl_3): δ = 19.61 (s, 1 H, Ru=CHPh), 7.99 (br. s, 1 H, pyridine), 7.57–6.38 (multiple peaks, 13 H, pyridine, *ortho* CH, *para* CH, *meta* CH, 2,6-dimethylphenyl aromatic CH), 4.16 (s, 2 H, $\text{NCH}_2\text{CH}_2\text{N}$), 3.95 (s, 2 H, $\text{NCH}_2\text{CH}_2\text{N}$), 2.75 (br. s, 9 H, pyridine CH₃, *ortho* CH₃), 2.24 (s, 6 H, *ortho* CH₃), 2.12 (s, 3 H, pyridine CH₃) ppm. ^{13}C NMR (CDCl_3 , 100 MHz): δ = 312.49 (m, Ru=CHPh), 218.38 [s, Ru–C(N)₂], 158.75, 151.24, 148.08, 140.46, 139.07, 137.86, 130.80, 130.15, 129.23, 128.89, 128.69, 128.53, 128.20, 126.01, 122.41, 51.63, 50.71, 31.51, 21.48, 20.45, 18.34 ppm.

[RuCl₂(=CHPh)(H₂Ime)(C₉H₇N₂)] (7): Isoquinoline (1.0 mL, 8.4 mmol) was added to complex **1** (0.30 g, 0.37 mmol) in a 150-mL Schlenk flask, then 5 mL of toluene was added as solvent. The reaction mixture was stirred at room temperature for 1 h, during which time a color change from red-brown to green was observed. Hexane (100 mL) was then added at room temperature and a green solid precipitated. The green precipitate was filtered, washed four times with 10 mL of hexane and dried in vacuo for 6 h to afford **7** as a green powder (0.14 g, 47% yield). ^1H NMR (400 MHz, CDCl_3): δ = 19.18 (s, 1 H, Ru=CHPh), 9.32 (s, 1 H, isoquinoline), 8.92 (s, 1 H, isoquinoline), 8.59 (s, 1 H, isoquinoline), 8.50 (s, 1 H, isoquinoline), 8.16–6.99 (multiple peaks, 21 H, isoquinoline, *ortho* CH, *para* CH, *meta* CH, 2,6-dimethylphenyl aromatic CH), 4.14 (s, 4 H, $\text{NCH}_2\text{CH}_2\text{N}$), 2.63 (br. s, 6 H, *ortho* CH₃), 2.35 (s, 6 H, *ortho* CH₃) ppm. ^{13}C NMR (CDCl_3 , 100 MHz): δ = 314.44 (m, Ru=CHPh), 218.31 [s, Ru–C(N)₂], 155.17, 152.80, 151.31, 150.52, 148.40, 144.56, 143.12, 138.17, 136.16, 135.73, 135.40, 131.45, 130.31, 130.13, 129.56, 128.94, 128.04, 127.90, 127.41, 127.22, 126.64, 126.46, 126.17, 121.18, 120.91, 120.40, 51.80, 20.45, 18.82 ppm.

X-ray Crystallographic Studies: Crystals suitable for X-ray diffraction were mounted on glass fibers. Data collection was performed

with a Bruker Smart APEX CCD diffractometer using graphite-monochromated Mo- K_{α} radiation ($\lambda = 0.71073 \text{ \AA}$) at 273 K (for complex **2**) or 180 K. The diffraction frames were integrated using the SAINT package. The structures were solved by direct methods using the program SHELXS-97. Structure refinements by full-matrix least squares on F^2 were carried out with the program SHELXL-97. All non-hydrogen atoms of the complexes were assigned anisotropic displacement parameters. The hydrogen atoms were constrained to idealized geometries and assigned isotropic displacement parameters equal to 1.2-times the U_{iso} values of their respective parent atoms. Crystal data and other details of the structure analyses are presented in Table 4. CCDC-635304 (**2**), -645279 (**6**), -642416 (**4**), -642417 (**5**), and -642415 (**7**) contain the supplementary crystallographic data for this paper. These data can be obtained free of charge from The Cambridge Crystallographic Data Center via www.ccdc.cam.ac.uk/data_request/cif.

Tandem Mass Spectrometry: The samples were delivered to the ionization source in $\text{CH}_2\text{Cl}_2/\text{CH}_3\text{CN}$ solution. The complexes were dissociated by collision-induced dissociation (CID) in the collision cell of a Micromass Q-ToF with a capillary voltage of 2300 V, an extraction cone voltage of 2 V, and a sample cone voltage of 10 V. The desolvation temperature was set to 190 °C and the source temperature to 100 °C. Nitrogen was used as both drying and nebulizing gas with flow rates of 450 and 50 L h^{-1} , respectively. The CID spectra were obtained by selecting the precursor ion of interest with the quadrupole and then collision with argon gas in the CID cell and finally mass analysis by ToF. The collision-cell pressure was maintained at 6 psi. Fragment ions were obtained upon adjusting the collision cone voltage of the mass spectrometer to higher values (for example 19 V).

General Procedure for Ring-Closing Metathesis: In a typical experiment, catalyst **4** (2.5 mg, 3.9 μmol) and diallylmalononitrile (117 mg, 0.8 mmol) were weighed into a dried, two-necked flask

equipped with a reflux condenser, and 8 mL of solvent was then added. The resulting mixture was then stirred under the conditions given in Table 2. After completion of the reaction, the mixture was filtered through a short pad of silica gel and the solvent removed in vacuo. Conversion was measured by GC-FID and confirmed by NMR spectroscopy. Compound **8**: $^1\text{H NMR}$ (400 MHz, CDCl_3): $\delta = 5.90$ (dd, $J = 7.2, 10.4, 16.8$ Hz, 2 H, $\text{CH}_2=\text{CHCH}_2$), 5.45 [dd, $J = 0.8, 10.4$ Hz, 2 H, (Z) $\text{CH}_2=\text{CHCH}_2$], 5.41 [dd, $J = 0.8, 16.8$ Hz, 2 H, (E) $\text{CH}_2=\text{CHCH}_2$], 2.69 (d, $J = 7.2$ Hz, 4 H, $\text{CH}_2=\text{CHCH}_2$) ppm. HRMS (EI): calcd. for $\text{C}_9\text{H}_{10}\text{N}_2$ [$\text{M}]^+$ 146.0844; found 146.0851. Compound **9**: $^1\text{H NMR}$ (400 MHz, CDCl_3): $\delta = 5.81$ (s, 2 H, $\text{CH}_2\text{CH}=\text{CHCH}_2$), 3.22 (s, 4 H, $\text{CH}_2\text{CH}=\text{CHCH}_2$) ppm. HRMS (EI): calcd. for $\text{C}_7\text{H}_6\text{N}_2$ [$\text{M}]^+$ 118.0531; found 118.0532.

General Procedure for the Cross Metathesis Reaction of Acrylonitrile with α -Olefins: In a typical experiment, catalyst **4** (16.4 mg, 25.9 μmol) was weighed into a dried, two-necked flask equipped with a reflux condenser, then 1-octene (290 mg, 2.6 mmol) and acrylonitrile (67 mg, 1.3 mmol) in CH_2Cl_2 (13 mL) were added. The resulting mixture was then stirred under the conditions listed in Table 3. After completion of the reaction, the mixture was filtered through a short pad of silica gel and the solvent removed in vacuo. The crude mixture was purified by chromatography on silica gel to yield the product (140 mg, 81%); the (E)/(Z) ratio was determined by $^1\text{H NMR}$ spectroscopy to be 1:2.8. Compound **10**: $^1\text{H NMR}$ (400 MHz, CDCl_3): $\delta = 6.69$ [dt, $J = 6.8, 16.4$ Hz, 1 H, (E) $\text{CH}_2\text{CH}=\text{CHCN}$], 6.47 [dt, $J = 7.6, 10.8$ Hz, 1 H, (Z) $\text{CH}_2\text{CH}=\text{CHCN}$], 5.30 [d, $J = 16.4$ Hz, 1 H, (E) $\text{CH}_2\text{CH}=\text{CHCN}$], 5.28 [d, $J = 10.8$ Hz, 1 H, (Z) $\text{CH}_2\text{CH}=\text{CHCN}$], 2.39 [q, $J = 7.6$ Hz, 2 H, (Z) $\text{CH}_2\text{CH}=\text{CHCN}$], 2.19 [q, $J = 6.8$ Hz, 2 H, (E) $\text{CH}_2\text{CH}=\text{CHCN}$], 1.26–1.31 (m, 8 H), 0.86 (t, $J = 6.8$ Hz, 3 H) ppm. Compound **11**: $^1\text{H NMR}$ (400 MHz, CDCl_3): $\delta = 6.71$ [dt, $J = 6.8, 16.4$ Hz, 1 H, (E) $\text{CH}_2\text{CH}=\text{CHCN}$], 6.49 [dt, $J = 7.6,$

Table 4. Crystallographic data for complexes **2** and **4–7**.

	2 · CHCl_3	4 · $2\text{CH}_2\text{Cl}_2$	5 · 3.25CHCl_3	6 · 2CHCl_3 · $0.5\text{H}_2\text{O}$	7 · 0.25CHCl_3 · $0.25\text{H}_2\text{O}$
Empirical formula	$\text{C}_{32}\text{H}_{34}\text{Cl}_5\text{N}_3\text{Ru}$	$\text{C}_{34}\text{H}_{39}\text{Cl}_6\text{N}_3\text{Ru}$	$\text{C}_{36.25}\text{H}_{40}\text{Cl}_{11.75}\text{N}_3\text{Ru}$	$\text{C}_{38}\text{H}_{41}\text{Cl}_8\text{N}_4\text{O}_{0.50}\text{Ru}$	$\text{C}_{44.25}\text{H}_{42.25}\text{Cl}_{2.75}\text{N}_4\text{O}_{0.25}\text{Ru}$
Formula mass	738.94	803.45	1035.32	946.42	832.65
Color	green	green	green	green	green
Crystal dimensions [mm]	$0.33 \times 0.14 \times 0.13$	$0.70 \times 0.40 \times 0.20$	$0.50 \times 0.25 \times 0.13$	$0.52 \times 0.50 \times 0.40$	$0.74 \times 0.60 \times 0.31$
Crystal system	triclinic	monoclinic	triclinic	triclinic	monoclinic
Space group	$P1$	$P2_1/c$	$P1$	$P1$	$P2_1/c$
a [Å]	10.1262(2)	11.1997(3)	9.3780(2)	9.9107(3)	12.1217(3)
b [Å]	11.0684(2)	15.4394(4)	12.5870(3)	12.3197(3)	18.3008(5)
c [Å]	14.8361(2)	21.0496(6)	19.7469(5)	17.1758(4)	19.8541(5)
α [°]	96.5600(10)	90	93.6080(10)	93.665(2)	90
β [°]	94.6810(10)	103.032(2)	100.3410(10)	90.712(2)	104.8440(10)
γ [°]	92.1950(10)	90	94.8690(10)	90.316(2)	90
V [Å ³]	1644.54(5)	3546.08(17)	2277.53(9)	2092.62(9)	4257.38(19)
Z	2	4	2	2	4
T [K]	273(2)	180(2)	180(2)	180(2)	180(2)
$D_{\text{calcd.}}$ [g cm^{-3}]	1.492	1.505	1.510	1.502	1.300
μ [mm^{-1}]	0.909	0.923	1.063	0.920	0.576
$F(000)$	752	1640	1045	962	1717
θ range [°]	2.35 to 29.07	2.29 to 25.00	1.63 to 25.00	2.63 to 25.00	2.06 to 25.00
Index ranges (h, k, l)	$\pm 13, \pm 15, \pm 20$	$\pm 13, \pm 18, -23$ to 25	$\pm 11, \pm 14, \pm 23$	-9 to 11, $\pm 14, \pm 20$	$\pm 14, \pm 21, \pm 23$
Reflections collected	18548	19876	18924	15278	45627
Independent reflections/ R_{int}	8678/0.0311	6219/0.0384	7949/0.0284	7301/0.0328	7481/0.0409
Obsd reflections [$I > 2\sigma(I)$]	6776	4944	6743	5600	6241
Data/restraints/parameters	8678/0/370	6219/0/397	7949/0/496	7301/3/464	7481/0/505
$R1/wR2$ [$I > 2\sigma(I)$]	0.0432/0.1058	0.0437/0.1167	0.0508/0.1548	0.0693/0.1972	0.0622/0.1994
$R1/wR2$ (all data)	0.0596/0.1157	0.0591/0.1257	0.0612/0.1638	0.0902/0.2136	0.0740/0.2078
GOF (on F^2)	1.034	1.048	1.086	1.059	1.098
Largest diff peak/hole [e \AA^{-3}]	1.520/−0.641	1.075/−1.184	1.452/−0.996	1.682/−1.455	1.502/−0.794

10.8 Hz, 1 H, (*Z*) CH₂CH=CHCN], 5.32 [d, *J* = 16.4 Hz, 1 H, (*E*) CH₂CH=CHCN], 5.30 [d, *J* = 10.8 Hz, 1 H, (*Z*) CH₂CH=CHCN], 2.42 [q, *J* = 7.6 Hz, 2 H, (*Z*) CH₂CH=CHCN], 2.22 [q, *J* = 6.8 Hz, 2 H, (*E*) CH₂CH=CHCN], 1.26–1.31 (m, 12 H), 0.89 (t, *J* = 6.8 Hz, 3 H) ppm.

Supporting Information (see footnote on the first page of this article): Tandem mass spectra of all complexes.

Acknowledgments

We thank Dr. Cheng He for X-ray crystallographic analysis and Prof. Xiao-Bing Lu, Dr. Xiao Jiang, Dr. Xiao-Gang Li, and Dr. Ping Liu for helpful discussions.

- [1] a) T. M. Trnka, R. H. Grubbs, *Acc. Chem. Res.* **2001**, *34*, 18–29; b) R. H. Grubbs, *Tetrahedron* **2004**, *60*, 7117–7140; c) A. Fürstner, *Angew. Chem.* **2000**, *112*, 3140–3172; *Angew. Chem. Int. Ed.* **2000**, *39*, 3012–3043; d) D. Astruc, *New J. Chem.* **2005**, *29*, 42–56; e) E. Colacino, J. Martinez, F. Lamaty, *Coord. Chem. Rev.* **2007**, *251*, 726–764.
- [2] M. Scholl, S. Ding, C. W. Lee, R. H. Grubbs, *Org. Lett.* **1999**, *1*, 953–956.
- [3] P. Schwab, R. H. Grubbs, J. W. Ziller, *J. Am. Chem. Soc.* **1996**, *118*, 100–110.
- [4] a) M. S. Sanford, M. Ulman, R. H. Grubbs, *J. Am. Chem. Soc.* **2001**, *123*, 749–750; b) M. S. Sanford, J. A. Love, R. H. Grubbs, *J. Am. Chem. Soc.* **2001**, *123*, 6543–6554.
- [5] M. S. Sanford, J. A. Love, R. H. Grubbs, *Organometallics* **2001**, *20*, 5314–5318.
- [6] J. A. Love, J. P. Morgan, T. M. Trnka, R. H. Grubbs, *Angew. Chem. Int. Ed.* **2002**, *41*, 4035–4037.
- [7] a) S. E. Lehman Jr, K. B. Wagener, *Organometallics* **2005**, *24*, 1477–1482; b) J. E. Williams, M. J. Harner, M. B. Sponsler, *Organometallics* **2005**, *24*, 2013–2015.
- [8] a) J. C. Conrad, D. Amoroso, P. Czechura, G. P. A. Yap, D. E. Fogg, *Organometallics* **2003**, *22*, 3634–3636; b) J. C. Conrad, H. H. Parnas, J. L. Snelgrove, D. E. Fogg, *J. Am. Chem. Soc.* **2005**, *127*, 11882–11883; c) S. Monfette, D. E. Fogg, *Organometallics* **2006**, *25*, 1940–1944; d) J. C. Conrad, K. Camm, D. E. Fogg, *Inorg. Chim. Acta* **2006**, *359*, 1967–1973.
- [9] D. Wang, L. Yang, U. Decker, M. Findeisen, M. R. Buchmeiser, *Macromol. Rapid Commun.* **2005**, *26*, 1757–1762.
- [10] W.-Z. Zhang, C.-X. Bai, X.-B. Lu, R. He, *J. Organomet. Chem.* **2007**, *692*, 3563–3567.
- [11] J. A. Love, M. S. Sanford, M. W. Day, R. H. Grubbs, *J. Am. Chem. Soc.* **2003**, *125*, 10103–10109.
- [12] a) M. S. Sanford, L. M. Henling, M. W. Day, R. H. Grubbs, *Angew. Chem. Int. Ed.* **2000**, *39*, 3451–3453; b) S. Takahashi, S. Hikichi, M. Akita, Y. Moro-oka, *Organometallics* **1999**, *18*, 2571–2573; c) D. J. Huang, K. Folting, K. G. Caulton, *J. Am. Chem. Soc.* **1999**, *121*, 10318–10322.
- [13] For representative examples of mass spectrometric studies on ruthenium catalysts, ruthenium-catalyzed olefin metathesis reactions, and tandem mass spectrometry in the gas phase, see: a) C. Adlhart, C. Hinderling, H. Baumann, P. Chen, *J. Am. Chem. Soc.* **2000**, *122*, 8204–8214; b) C. Adlhart, P. Chen, *Angew. Chem. Int. Ed.* **2002**, *41*, 4484–4487; c) P. Chen, *Angew. Chem. Int. Ed.* **2003**, *42*, 2832–2847; d) P. Chen, M. H. Chisholm, J. C. Gallucci, X.-Y. Zhang, Z.-P. Zhou, *Inorg. Chem.* **2005**, *44*, 2588–2595.
- [14] W.-Z. Zhang, R. Zhang, R. He, *Tetrahedron Lett.* **2007**, *48*, 4203–4205.
- [15] E. Díez-Barra, A. de la Hoz, A. Moreno, P. Sánchez-Verdú, *J. Chem. Soc. Perkin Trans. 1* **1991**, 2589–2592.

Received: June 18, 2007

Published Online: October 8, 2007